

N71-15973

SPACE RESEARCH COORDINATION CENTER

NASA CR116142



# GAS PHASE REACTION RATES OF SOME POSITIVE IONS WITH WATER AT 296° K

BY

C.J. HOWARD, H.W. RUNDLE AND  
F. KAUFMAN

DEPARTMENT OF CHEMISTRY

SRCC REPORT NO. 131

UNIVERSITY OF PITTSBURGH  
PITTSBURGH, PENNSYLVANIA

19 OCTOBER 1970

CASE FILE  
COPY

The Space Research Coordination Center, established in May, 1963, has the following functions: (1) it administers predoctoral and postdoctoral fellowships in space-related science and engineering programs; (2) it makes available, on application and after review, allocations to assist new faculty members in the Division of the Natural Sciences and the School of Engineering to initiate research programs or to permit established faculty members to do preliminary; work on research ideas of a novel character; (3) in the Division of the Natural Sciences it makes an annual allocation of funds to the interdisciplinary Laboratory for Atmospheric and Space Sciences; (4) in the School of Engineering it makes a similar allocation of funds to the Department of Metallurgical and Materials Engineering and to the program in Engineering Systems Management of the Department of Industrial Engineering; and (5) in concert with the University's Knowledge Availability Systems Center, it seeks to assist in the orderly transfer of new space-generated knowledge in industrial application. The Center also issues periodic reports of space-oriented research and a comprehensive annual report.

The Center is supported by an Institutional Grant (NsG-416) from the National Aeronautics and Space Administration, strongly supplemented by grants from the A. W. Mellon Educational and Charitable Trust, the Maurice Falk Medical Fund, the Richard King Mellon Foundation and the Sarah Mellon Scaife Foundation. Much of the work described in SRCC reports is financed by other grants, made to individual faculty members.

# GAS PHASE REACTION RATES OF SOME POSITIVE IONS WITH WATER AT 296°K\*

Carleton J. Howard<sup>†</sup>, Howard W. Rundle, and Frederick Kaufman

Department of Chemistry  
University of Pittsburgh  
Pittsburgh, Pa. 15213

## Abstract

Measurements of the rate constants for the reactions of  $\text{He}^+$ ,  $\text{Ne}^+$ ,  $\text{Ar}^+$ ,  $\text{Kr}^+$ ,  $\text{O}^+$ ,  $\text{N}^+$ , and  $\text{N}_2^+$  with  $\text{H}_2\text{O}$  by the flowing afterglow technique at 296°K gave values of 0.56, 0.74, 1.43, 1.19, 2.33, 2.57, and  $2.19 \times 10^{-9}$   $\text{cm}^3/\text{sec}$  with standard deviation of 7 to 15%. They are in good agreement with extrapolated beam results for  $\text{Ar}^+$ ,  $\text{O}^+$ ,  $\text{N}^+$ , and  $\text{N}_2^+$ . Close agreement is also found for all but  $\text{He}^+$  and  $\text{Ne}^+$  with estimates based on classical trajectory calculations for similar ion plus dipole systems.

## I. Introduction

Rapid progress has recently been made in the measurement of ion-neutral reaction rates, especially at low energies, utilizing steady-state flow techniques, as applied to these reactions with particular success by Ferguson and coworkers<sup>1,2</sup> at ESSA. Such data are needed for an understanding of normal or perturbed planetary ionospheres, they may find application in chemi-ionization connected with combustion processes, and their collection and interpretation represents a major advance in one of the last unexplored areas in the field of chemical transformation of simple species.

In this paper, we report rate constants for the reactions of one molecular and six atomic ions with  $H_2O$  using the flowing afterglow technique and making sure that  $H_2O$  concentrations are measured with sufficient accuracy ( $\pm 5\%$ ) even though these concentrations are in the range  $10^{11}$  to  $10^{13}$   $cm^{-3}$  in the flow tube. This has been a serious impediment to such studies in the past and accounts for the paucity of quantitative data for reactions involving water vapor. The extension of the present work to include ion cluster formation and reaction rate constants for aeronomically important ions such as  $O_2^+$ ,  $NO^+$ , and  $H_3O^+$  is now under way. These clustered ions have been identified as major species in the D-region of the ionosphere in sounding rocket experiments<sup>3</sup>, and have also been studied in laboratory experiments<sup>4,5</sup>. The overall bimolecular rate constants reported here represent pure charge-transfer in three cases and charge-transfer plus one or more rearrangement processes in the other four. Although a sufficiently detailed theory of the collisional interaction of ions with non-linear molecules having large dipole moments is not yet available, it is of interest to compare the present results with calculations based on some simple models.

## II. Experimental

The apparatus is shown schematically in Fig. 1. Several modifications of a previously described version<sup>6</sup> will be discussed in this section.

The helium carrier gas (80 to 360 std cc/sec) enters the reaction tube through the off axis branch of a 3 in. i.d. Pyrex Y (Corning drainline) sealed onto the tube. This prevents uv radiation from the ion source from producing ions or excited species in the reaction zone and facilitates the addition of reactants or other precursor gases at variable positions.

Primary ions can be produced either in a microwave discharge or by electron impact. The latter method was used exclusively in this work. The ionizer consists of a 0.5 in. length of coiled 0.005 in. diam. thoria-coated iridium wire mounted on-axis in the sidearm of the Y tube. The iridium filament is surrounded at a distance of 5 mm by a cylindrical grid which is maintained at ground potential and the ionizing electrons are accelerated by operating the filament at a negative potential between 30 and 110 volts. The electrons are collected on a concentric, gold-plated brass cylinder mounted snugly in the tube. The ionizer is powered by a regulated supply (Extranuclear Laboratories Electron Energy and Emission Control, Type II) operated in the constant emission current mode. The emission current, variable from 0 to 20 ma, is normally 1 ma. Reactant ions can be formed by adding gases before or after the ionizer.

The reaction tube pressure is measured by a pressure transducer (Pace Engineering Co. Model P7D,  $\pm 0.1$  p.s.i. and Model CD25 Indicator) calibrated with a McLeod gauge. Pressure measurements were corrected, when necessary, for the pressure drop along the flow tube and represent an average pressure in the reaction zone.

At the downstream end of the reaction tube the ions pass through the on-axis sampling orifice at the tip of one of three interchangeable molybdenum cones 0.5 in. diam. at the base. These cones have orifices of 0.18, 0.31, and 0.65 mm diam.; the 0.31 mm cone was used in this work. The cone assembly is electrically insulated from ground and can be held at any desired potential. In the present work, all sampling was done at ground potential.

Mass discrimination of the ions sampled from the plasma can occur at

the sampling orifice, in the ion accelerating and focusing system, in the quadrupole mass filter, and at the electron multiplier. However, mass discrimination does not affect the measurement of the rate constants reported here since only the parent ion current is involved in the calculations.

Precursor or reactant gases can be added at variable positions in the reaction tube through either of two movable injectors consisting of multi-perforated rings of teflon tubing attached to the ends of stainless steel tubes. The neutral reactant, water vapor, is added through the downstream injector which is movable over a distance of 70 cm. The distance between the sampling orifice and this injector defines the reaction zone and is measured accurately on an external scale not shown in the diagram. The teflon ring provides a planar source of added reactant in the flow tube, an addition mode which is preferable over the usual fixed point sources both for simplification of flow analysis and for ease of doing experiments at variable distance of added reactant. Planarity was checked by adding some NO through the injector to a stream of helium containing N or O atoms produced in the microwave discharge cavity and by observing the spatial distribution of the light from the chemiluminescent  $O + NO$  (air afterglow) recombination.

The source of added water vapor is a flask containing liquid water in equilibrium with its vapor at a temperature preset in the range  $70^{\circ}$  to  $95^{\circ}C$  to within  $\pm 0.1^{\circ}$  by a thermoregulator. The water flow rate is controlled by the temperature setting and by a stainless steel needle valve. The arm of the flask up to and including the needle valve is heated to about  $100^{\circ}C$  to prevent condensation. The water vapor flow is then mixed with a flow of helium (0.1 to 0.5 std cc/sec) which is measured with a calibrated flow-

meter (Brooks Sho-rate floating ball type). After mixing, the He-H<sub>2</sub>O mixture is passed through a 3 in. section of copper pipe (1.5 in. i.d.) where the total pressure is measured by a pressure transducer (Pace Engineering Co. Model P7D, ±0.2 p.s.i. and Model CD25 Indicator) and the partial pressure of water is measured with a hygrometer (Panametrics Model 1000) which is sensitive only to water vapor and is capable of measuring partial pressures over a wide range (10<sup>-4</sup> to 10 torr). However, the hygrometer was found to have two operating difficulties: (1) a very slow time response (about 20 min.) at water vapor pressures less than about 0.1 torr and (2) a calibration which was somewhat unreliable over an extended period of time. The latter problem manifested itself as a parallel displacement of the calibration curve depending on the preceding history of the probe environment. It was therefore preferable to recalibrate two or three points each day and hence assure an accurate calibration by direct measurement of pure H<sub>2</sub>O in the cell using both the hygrometer and the pressure transducer. Moreover, this calibration was further checked at several points under typical operating conditions by passing the H<sub>2</sub>O-He mixture through a small trap immersed in liquid N<sub>2</sub> and weighing the water collected over a known length of time. The two methods agree to within about ±3% and H<sub>2</sub>O concentrations are probably accurate to within 5%.

The flow of water,  $F_{H_2O}$ , is calculated from the known helium flow,  $F_{He}$ , the total pressure in the measuring cell,  $P$ , and the partial pressure of water vapor in the measuring cell,  $P_{H_2O}$ , by the relation

$$F_{H_2O} = F_{He} \left( \frac{P_{H_2O}}{P - P_{H_2O}} \right).$$

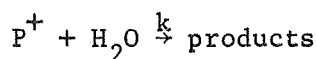
The He-H<sub>2</sub>O mixture is then added to the reaction tube through the downstream movable injector.

Ion currents and the H<sub>2</sub>O partial pressure are recorded simultaneously on a dual pen strip chart recorder (Texas Instruments Model P502W6A).

### III. Data Analysis

The data analysis for ion-molecule flow systems has been discussed in detail elsewhere<sup>1,7-9</sup>. The analysis used here is identical to that derived by Huggins and Cahn<sup>7</sup> which is in excellent agreement with the results presented by Ferguson et al.<sup>1</sup>

For the reaction



a reasonable model of the flowing afterglow system requires a solution of the equation

$$2\bar{v} \{ 1 - (r/R)^2 \} \frac{\partial [P^+]}{\partial z} = \frac{D_{P^+}}{r} \left\{ \frac{\partial}{\partial r} (r \frac{\partial [P^+]}{\partial r}) \right\} - k [P^+][H_2O] \quad (1)$$

where  $\bar{v}$  is the average stream velocity,  $r$  the radial distance from the tube axis,  $R$  the tube radius,  $z$  the axial coordinate, and  $D_{P^+}$  the ambipolar diffusion coefficient of  $P^+$ . Equation (1) incorporates the following major assumptions: (1) laminar flow exists in the tube, (2) axial diffusion of the ions is neglected, (3) volume recombination of the ions is an unimportant loss mechanism, (4) source terms of  $P^+$  are insignificant in the reaction zone, (5) the concentration of added H<sub>2</sub>O is radially uniform, and (6) the reaction zone begins sufficiently far downstream that only the lowest diffusion mode needs to be considered. The solution of the equation<sup>7</sup> employs a variational



technique and leads, in good approximation, to the simple relation

$$\ln [P^+] = C - \frac{k [H_2O] z}{\alpha \bar{v}} \quad (2)$$

where C is a constant and  $\alpha$  is a correction factor. A simple one-dimensional treatment neglecting diffusion yields a similar result with  $\alpha = 1$  and thus one multiplies the apparent rate constant obtained from the simplest model by  $\alpha$ . Huggins and Cahn<sup>7</sup> obtained  $\alpha = 1.59$ . More recently, Bolden et al.<sup>8</sup> took into account slip flow at the wall of the reaction tube, i.e. a modification of approximation (1), which at the lowest pressures (0.2 torr) leads to a decrease in  $\alpha$  of about 4%. If axial diffusion were taken into account this would tend to increase  $\alpha$ . A simple one-dimensional treatment of axial diffusion ignoring the velocity profile produces a correction of  $k'D_p/\bar{v}^2$ <sup>10</sup> where  $k'$  is the pseudo first order rate constant calculated from the logarithmic concentration decrease. Substitution of typical values produces an increase in  $\alpha$  of about 2 - 6%. Thus, neglecting both slip flow and axial diffusion as was done in the earlier derivations of Huggins and Cahn<sup>7</sup> and of Farragher<sup>9</sup> will not produce a significant error as these effects tend to cancel, and a value of  $\alpha = 1.59$  was therefore used in this work.

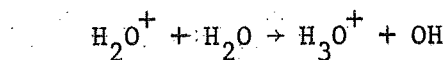
The rate constants can thus be obtained by plotting  $\log [P^+]$  either vs.  $z$  at constant  $F_{H_2O}$  or vs.  $F_{H_2O}$  at constant  $z$ . Good agreement was obtained using these two techniques.

#### IV. Results

Typical plots of the decay of the parent ion,  $Ar^+$ , as a function of the injector position at constant  $H_2O$  concentration are shown in Fig. 2, and as

a function of  $\text{H}_2\text{O}$  concentration at constant injector position in Fig. 3. The problem of collecting data by varying the  $\text{H}_2\text{O}$  concentration is evident in Fig. 3 where the scatter of the points along the line is due to drifts occurring during the long time required to obtain each hygrometer reading. Measurements made by moving the injector or by varying the  $\text{H}_2\text{O}$  concentration yielded equal rate constants within experimental scatter in all cases, but because of its greater speed and reliability, the former method was used for collecting most of the data.

In all of the reactions studied,  $\text{H}_2\text{O}^+$  is a primary product ion and in some cases  $\text{PH}^+$  ( $\text{P}^+$  = parent ion) and  $\text{OH}^+$  are primary products as well. These primary product ions react rapidly with  $\text{H}_2\text{O}$ . For example, for the charge transfer product,  $\text{H}_2\text{O}^+$ , the reaction



has a rate constant of about  $1.7 \times 10^{-9}$  cc/sec<sup>5,11</sup>. Hydronium ion is also produced by the rapid proton transfer reactions of  $\text{OH}^+$  and  $\text{PH}^+$  with  $\text{H}_2\text{O}$  and thus always appears as the dominant ion product after the parent ions have reacted to completion. Further increase in water concentration results in the appearance of water cluster ions of the type  $\text{H}_3\text{O}^+ (\text{H}_2\text{O})_n$ . With  $\text{He}^+$  and  $\text{Ne}^+$  there are at least 7 and 5 energetically accessible reaction branches, respectively, and Fig. 4 shows an experiment in which all of the ions were monitored for the reaction of  $\text{He}^+$  with  $\text{H}_2\text{O}$ . In this example the  $\text{H}_2\text{O}$  concentration was low ( $\sim 6 \times 10^{11}$  molecules/cc) so that reasonable concentrations of primary product ions could be seen. The ion currents at  $z = 0$  are the background signals obtained when no water is added through the movable injector and the dashed curves between  $z = 0$  and  $z = 16$  cm are interpolated, as no measurements were made for  $z < 16$  cm.

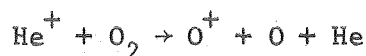
No attempt was made to obtain quantitative branching ratios for those reactions with more than one energetically possible channel. Such ratios could be obtained from the axial profiles of the primary product ions only if the rate constants for their reactions with  $H_2O$  were actually known, but such is not the case for the proton transfer reactions. As can be seen from Fig. 4, moderate amounts (5 to 10% of  $[P^+]$ ) of product ions are present in the system even in the absence of added  $H_2O$ . These ions are formed by the reaction of the parent ion with water vapor from the surfaces of the system. Small amounts of other impurity ions ( $N^+$ ,  $N_2^+$ ,  $Ne^+$ ,  $O^+$ ) are also present, as are some metastable excited neutral species ( $He\ 2\ ^3S$ ) which react with  $H_2O$  to produce the same product ions formed in the reaction being studied. It should be stressed, however, that these complications do not affect the results reported here and lead to difficulty only in the determination of branching ratios.

A summary of the measured total bimolecular rate constants is given in Table I. Each rate constant represents an average of a number of experiments in which the total pressure was varied from 0.3 to 1 torr and the concentration of  $H_2O$  was varied over a factor of 4. The standard deviations of the rate constants lie between 7 and 15% of the average, but an overall accuracy of only  $\pm$  (20 - 30%) is claimed. The reactions are described in greater detail in the following sections.

A.  $O^+$ ,  $N^+$ ,  $N_2^+$

An  $O^+$  plasma was prepared by adding a small flow of  $O_2$  (<0.04% of total flow) either before or after the ionizer. The measured rate constant was found to be independent of the point of addition. The major source of  $O^+$  in

both cases is the dissociative charge transfer reaction

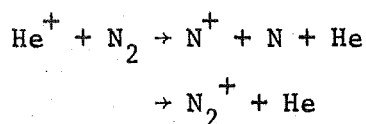


which has a rate constant of about  $1 \times 10^{-9}$  cc/sec.<sup>12,13</sup>

The reaction of  $\text{O}^+$  with  $\text{H}_2\text{O}$  is exothermic only for the charge transfer channel



The reactions of  $\text{N}^+$  and  $\text{N}_2^+$  with  $\text{H}_2\text{O}$  were studied simultaneously in a plasma produced by the reaction of  $\text{He}^+$  with  $\text{N}_2$  (<1.0% of total flow) added either before or after the ionizer.

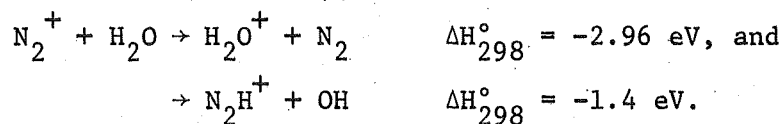


The rate constants for these reactions are about  $6 \times 10^{-10}$  cc/sec and  $4 \times 10^{-10}$  cc/sec respectively<sup>13,15</sup>. The reaction with  $\text{N}^+$  was found to proceed entirely by the charge transfer mechanism



The H atom transfer and  $\text{H}^-$  ion transfer reactions are both slightly endothermic (about 0.04 and 0.09 eV respectively) and the products  $\text{NH}^+$  and  $\text{OH}^+$  were not observed.

There are two possible channels for the reaction of  $\text{N}_2^+$  with  $\text{H}_2\text{O}$ ,



Both ionic products,  $\text{N}_2\text{H}^+$  and  $\text{H}_2\text{O}^+$ , were observed.

The "tailing-off" of the  $\text{N}_2^+$  signals at large concentrations of  $\text{H}_2\text{O}$  and long reaction times (see Fig. 5) can be attributed to a breakdown of the assumption that source terms of the parent ion are not important in the reaction zone. In this case, the source of  $\text{N}_2^+$  could be reasonably attributed to

Penning ionization of  $N_2$  by  $He(2^3S)$  whose rate constant is  $7 \times 10^{-11} \text{ cm}^3 \text{ sec}^{-1}$ . The fact that  $N^+$  did not exhibit the tailing-off in the same experiment supports this explanation, since the formation of  $N^+$  from  $He(2^3S)$  and  $N_2$  is not energetically possible.

B.  $He^+$ ,  $Ne^+$ ,  $Ar^+$ ,  $Kr^+$

The rare gas ions were formed by direct ionization in the electron impact ionizer and Penning ionization by helium metastables. Small flows of Ne (0.5 to 7%), Ar (about 10%), and Kr (0.5 to 2%) were added to the main He flow for preparation of their respective plasmas.

The reaction of  $He^+$  with  $H_2O$  has a least seven possible channels (not considering the formation of products in excited states):

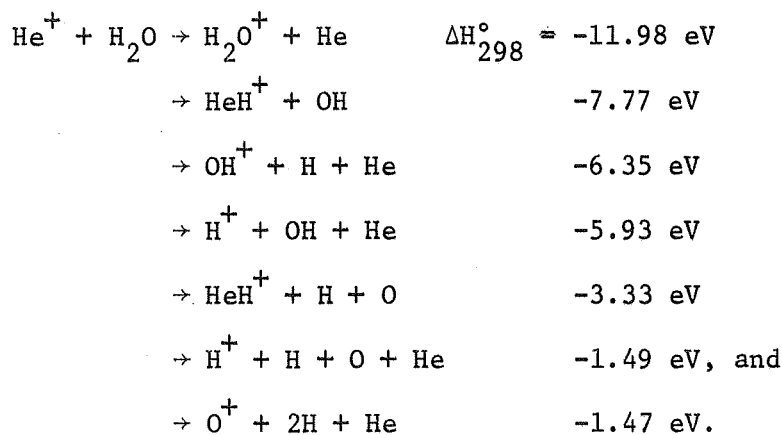
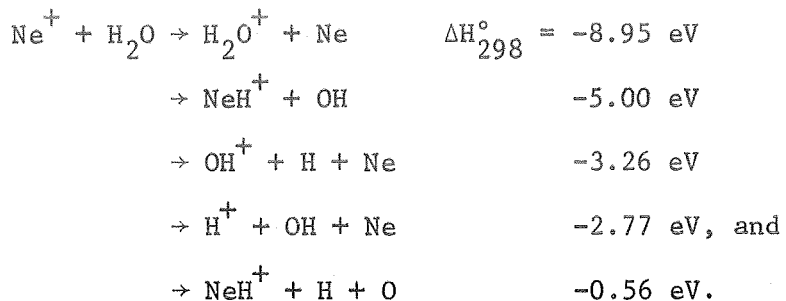
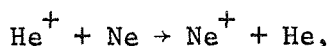


Fig. 4, which has been discussed previously, shows that the main primary products produced in this reaction are  $H_2O^+$ ,  $OH^+$ , and  $HeH^+$ , and that  $H^+$  and  $O^+$  are not formed in significant amounts. A simple computer calculation of the consecutive reactions including the disappearance of the primary products by proton transfer with  $H_2O$  demonstrated semi-quantitative agreement with the observed magnitude of  $H_3O^+$  as a secondary product.

The energetically possible reactions for  $Ne^+$  are

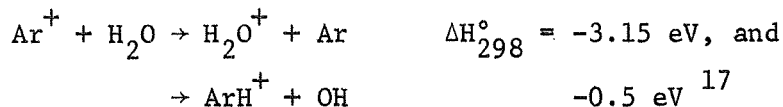


Because of limitations on the available quantity of Ne, experiments analogous to that of Fig. 4 were not done.  $\text{NeH}^+$  was observed, however, in small concentrations and was rapidly removed by proton transfer with  $\text{H}_2\text{O}$ . When the concentration of  $\text{H}_2\text{O}$  was greater than about  $1.5 \times 10^{12}$  molecules/cc a tailing-off of the  $\text{Ne}^+$  ion signal was observed similar to that previously described for  $\text{N}_2^+$ . This can be explained by the reaction



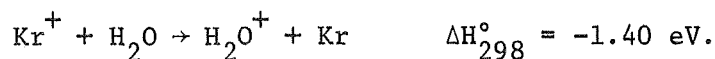
if its rate constant is not too much below its estimated upper limit of  $10^{-13}$  cc/sec<sup>12</sup>.

For  $\text{Ar}^+$  the only exothermic reactions are



and both product ions were observed.

The rate constant determined for  $\text{Kr}^+$  pertains entirely to the charge transfer channel

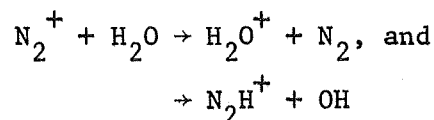


The formation of  $\text{KrH}^+$  by H atom transfer from  $\text{H}_2\text{O}$  to  $\text{Kr}^+$  is endothermic by about 1 eV but a small peak at mass 85 was observed which can not be attributed to a Kr isotope and which increased in intensity as small amounts of water were added to the  $\text{Kr}^+$  plasma. More than 97% of natural Kr is in the form of 4 isotopes,  $^{82}\text{Kr}$  (11.6%),  $^{83}\text{Kr}$  (11.6%),  $^{84}\text{Kr}$  (56.9%), and  $^{86}\text{Kr}$

(17.4%), and the peak at mass 85 probably was  $^{84}\text{KrH}^+$  formed by a proton transfer reaction of Kr with  $\text{HeH}^+$ . Measurements of the  $\text{Kr}^+-\text{H}_2\text{O}$  charge transfer reaction rate constant were made by monitoring the peak at mass 84 where  $^{83}\text{KrH}^+$  could interfere and at mass 86 where there can be no interference. Agreement to within the reported standard deviation was obtained and the value reported is an average of both kinds of data.

## V. Discussion

There is a dearth of experimental measurements of rate constants of ion- $\text{H}_2\text{O}$  reactions at thermal energies. The reactions



have been studied in a corona discharge by Shahin<sup>18</sup> who reported rate constants of  $9.5 \times 10^{-11}$  and  $9.5 \times 10^{-10}$  cc/sec respectively. These are to be compared with a total rate constant measured here of  $2.19 \times 10^{-9}$  cc/sec. In the corona discharge, Shahin estimated that the ions could have energies up to about 0.6 eV.

There is some evidence that the cross section of such reactions has an energy dependence which lies between  $\epsilon^{-0.5}$  and  $\epsilon^{-1}$  and that the rate constant would therefore exhibit a small negative energy dependence which would bring Shahin's and our data into qualitative agreement. It is disturbing, however, that Shahin reports charge transfer to account for only 10% of the total reaction, because this would require that charge transfer be more than 10 times faster for  $\text{O}^+$  and  $\text{N}^+$  (where it is the only available channel), than for  $\text{N}_2^+$ , even though the three overall rate constants are of very similar magnitude. The alternate explanation that charge transfer and atom transfer have very

different energy dependences seems unlikely in view of Turner and Rutherford's<sup>19</sup> beam experiments. These authors studied charge transfer of  $N^+$ ,  $O^+$ ,  $N_2^+$ , and  $Ar^+$  with  $H_2O$  over the energy range 1.5 to 400 eV and reported cross sections of 15, 20, 50, and  $25\text{\AA}^2$ , respectively for the four reactions at 2.0 eV ion energy. All four reactions show a negative energy dependence at the low energy end of the range, and if an  $\epsilon^{-1/2}$  extrapolation is assumed for the cross sections below 2 eV, energy-independent rate constants of 0.7, 1.0, 1.9, and  $0.8 \times 10^{-9} \text{ cm}^3/\text{sec}$  are obtained, in good agreement with the present results for  $N_2^+$  and  $Ar^+$ , where atom-transfer channels also contribute in our experiments, but substantially too low for  $N^+$  and  $O^+$ . A somewhat stronger negative energy dependence which is suggested by Dugan and Magee<sup>20</sup> and by Dugan<sup>21</sup> would further increase the extrapolated rate constants and lead to generally fair agreement with the present results, but not with Shahin's value for the  $N_2^+$  charge transfer rate constant.

Other relevant experimental studies include Stockdale, Compton, and Reinhardt's<sup>22</sup> recent measurements of the  $H^- + H_2O$  and  $D^- + D_2O$  proton or deuteron transfer reaction at ion energies of thermal to 3.6 eV which show a negative energy dependence of about  $\epsilon^{-1}$  for the cross section, but exceed in magnitude Dugan's<sup>21</sup> calculated cross section which is discussed below. A great deal of experimental work has been done on the proton transfer reactions  $H_2O^+ + H_2O$  and  $OH^+ + H_2O$  mentioned earlier whose rate constants are between 1.5 and  $2.0 \times 10^{-9} \text{ cm}^3/\text{sec}$ .

For a comparison with simple classical theories, one may begin with the Langevin ion-induced dipole interaction which leads to the well-known energy-independent rate constant<sup>23</sup>,  $k_L = 2\pi (e^2 \alpha/m)^{1/2}$ , where  $\alpha$  is the polarizability of the neutral reactant and  $m$  the reduced mass of the en-



counter. Calculated values of  $k_L$ , which differ only in  $m$ , are shown in column 4 of Table I. If an ion-permanent dipole interaction is added to the Langevin term and the dipole is assumed to remain "locked" into its lowest energy orientation, a rate constant,  $k_M$ , is obtained<sup>11,24</sup> larger than  $k_L$  by the term  $2\epsilon\mu \left(\frac{2\pi}{mkT}\right)^{1/2}$  where  $\mu$  is the permanent dipole moment. Calculated values of  $k_M$  are shown in column 5 of Table I ( $\alpha = 1.44 \times 10^{-24} \text{ cm}^3$ ,  $\mu = 1.85 \text{ Debye}$ ). Except for  $\text{He}^+$  and  $\text{Ne}^+$ , where the exothermicity is very large and where the classical approximation is likely to break down,  $k_L$  underestimates the rate constant by a factor of about two, and  $k_M$  overestimates it about threefold. Since  $k_M$  is an upper limit, i.e. the dipole can not be expected to remain aligned during the collision, the measured  $k$ 's are quite reasonable. For  $\text{N}^+$ ,  $\text{O}^+$ , and  $\text{N}_2^+$ , the relative magnitudes closely follow the simple  $m^{-1/2}$  dependence, though this agreement may be fortuitous.

Further comparison can be made with Dugan and Magee's<sup>20</sup> classical trajectory calculations of ion + HCl encounters where the reaction probability is obtained as the fraction of collision trajectories for which ion and molecule approach to within  $2\text{\AA}$ . The calculated cross section was found to be 30% larger than the Langevin cross section for HCl and to be about linear in  $\mu$ , based on calculations for  $\text{CH}_3 \text{CN}$ <sup>25</sup>. Applying this correction one would expect the  $\text{H}_2\text{O}$  reaction to be about twice as fast as  $k_L$ , in good qualitative agreement with experiment.

In connection with the laboratory studies of the  $\text{H}^- + \text{H}_2\text{O}$  reaction Dugan<sup>21</sup> has calculated a cross section of  $110\text{\AA}^2$  for an  $\text{H}^-$  energy of 0.2 eV and thermal rotational and vibrational energy of  $\text{H}_2\text{O}$ . Using his calculated dependence of  $\epsilon^{-0.65}$  for the cross section one obtains a rate constant of  $9 \times 10^{-9} \text{ cm}^3/\text{sec}$  at 300°K and, by the usual  $m^{-1/2}$  correction, 3.2, 3.0, and

$2.6 \times 10^{-9} \text{ cm}^3/\text{sec}$  for the  $\text{N}^+$ ,  $\text{O}^+$ , and  $\text{N}_2^+$  reactions, in very good agreement with our experimental results.

The rare gas ion sequence is dominated by the large deviations of  $\text{He}^+$  and  $\text{Ne}^+$  from simple classical behavior, similar to their abnormally slow reactions with some non-polar molecules<sup>8,26</sup>.  $\text{Ar}^+$  and  $\text{Kr}^+$  are only moderately below their calculated classical rate constants and apparently follow the expected mass dependence.

## References

\* This research was supported by the Advanced Research Projects Agency, The Department of Defense, and was monitored by U. S. Army Research Office - Durham, Box CM, Durham, N. C. 27706, under Contract No. DA-31-124-ARO-D-440.

† National Science Foundation Trainee. This work will be submitted in partial fulfillment of the requirements for the degree of Doctor of Philosophy at the University of Pittsburgh.

1. E. E. Ferguson, F. C. Fehsenfeld, and A. L. Schmeltekopf, Advan. At. and Mol. Phys., (Academic Press, N. Y., 1969), Vol. 5.
2. F. C. Fehsenfeld, A. L. Schmeltekopf, D. B. Dunkin, and E. E. Ferguson, ESSA Technical Report ERL 135-AL 3 (1969).
3. R. S. Narcisi and A. D. Bailey, J. Geophys. Res. 70, 3687 (1965); R. S. Narcisi, Planetary Electrodynamics (Gordon and Breach, N. Y., 1969), Vol. 2, p. 69.
4. A. Good, D. A. Durden, and P. Kebarle, J. Chem. Phys. 52, 222 (1970); W. C. Lineberger and L. J. Puckett, Phys. Rev. 187, 286 (1969).
5. A. Good, D. A. Durden, and P. Kebarle, J. Chem. Phys. 52, 212 (1970).
6. A. L. Farragher, J. A. Peden, and W. L. Fite, J. Chem. Phys. 50, 287 (1969).
7. R. W. Huggins and J. H. Cahn, J. Appl. Phys. 38, 180 (1967).
8. R. C. Bolden, R. S. Hemsworth, M. J. Shaw, and N. D. Twiddy, J. Phys. B: Atom. Molec. Phys. 3, 45 (1970).
9. A. L. Farragher, Trans. Faraday Soc., 66, 1411 (1970).
10. F. Kaufman, Progress in Reaction Kinetics (Pergammon Press, N. Y., 1961), Vol. 1, p. 12.
11. S. K. Gupta, E. G. Jones, A. G. Harrison, and J. J. Myer, Can. J. Chem. 45, 3107 (1967).
12. F. C. Fehsenfeld, A. L. Schmeltekopf, P. D. Goldan, H. I. Schiff, and E. E. Ferguson, J. Chem. Phys. 44, 4087 (1966).
13. J. Heimerl, R. Johnsen, and M. A. Biondi, J. Chem. Phys. 51, 5041 (1969) and references quoted therein.
14. Reaction enthalpies are calculated from data given in J. L. Franklin, J. G. Dillard, H. M. Rosenstock, J. T. Herron, K. Draxl, and F. H. Field, Ionization Potentials, Appearance Potentials, and Heats of Formation of Gaseous Positive Ions (U. S. Department of Commerce,

Washington, D. C., 1969), NSRDS-NBS 26.

15. D. B. Dunkin, F. C. Fehsenfeld, A. L. Schmeltekopf, and E. E. Ferguson, *J. Chem. Phys.* 49, 1365 (1968).
16. R. C. Bolden, R. S. Hemsworth, M. J. Shaw, and N. D. Twiddy, *J. Phys. B: Atom. Molec. Phys.* 3, 61 (1970).
17. This value was calculated using a proton affinity of 3.4 eV for Ar from W. A. Chupka and M. E. Russell, *J. Chem. Phys.* 49, 5426 (1968).
18. M. M. Shahin, *J. Chem. Phys.* 47, 4392 (1967).
19. B. R. Turner and J. A. Rutherford, *J. Geophys. Res.* 73, 6751 (1968).
20. J. V. Dugan, Jr. and J. L. Magee, *J. Chem. Phys.* 47, 3103 (1967).
21. J. V. Dugan, Jr., private communication.
22. J. A. D. Stockdale, R. N. Compton, and P. W. Reinhardt, *Phys. Rev.* 184, 81 (1969).
23. G. Gioumouisis and D. P. Stevenson, *J. Chem. Phys.* 29, 294 (1958).
24. T. F. Moran and W. H. Hamill, *J. Chem. Phys.* 39, 1413 (1963).
25. J. V. Dugan, Jr., J. H. Rice, and J. L. Magee, *Chem. Phys. Letters* 3, 323 (1969).
26. R. S. Hemsworth, R. C. Bolden, M. J. Shaw, and N. D. Twiddy, *Chem. Phys. Letters* 5, 237 (1970).

Table I. Rate Constants.

Reaction	Number of Experiments	k (cc/molecule sec) x 10 <sup>9</sup>		
		Experimental	$\frac{k_L^{(a)}}{L}$	$\frac{k_M^{(a)}}{M}$
O <sup>+</sup> + H <sub>2</sub> O	11	2.33 ± .25 <sup>(b)</sup>	.97	6.7
N <sup>+</sup> + H <sub>2</sub> O	16	2.57 ± .4	1.0	7.0
N <sub>2</sub> <sup>+</sup> + H <sub>2</sub> O	13	2.19 ± .3	.85	5.9
He <sup>+</sup> + H <sub>2</sub> O	20	0.56 ± .05	1.6	11
Ne <sup>+</sup> + H <sub>2</sub> O	7	0.74 ± .08	.91	6.4
Ar <sup>+</sup> + H <sub>2</sub> O	11	1.43 ± .1	.80	5.6
Kr <sup>+</sup> + H <sub>2</sub> O	12	1.19 ± .2	.73	5.1

(a) These are theoretical rate constants defined in the text.

(b) The limits represent one standard deviation from the mean.

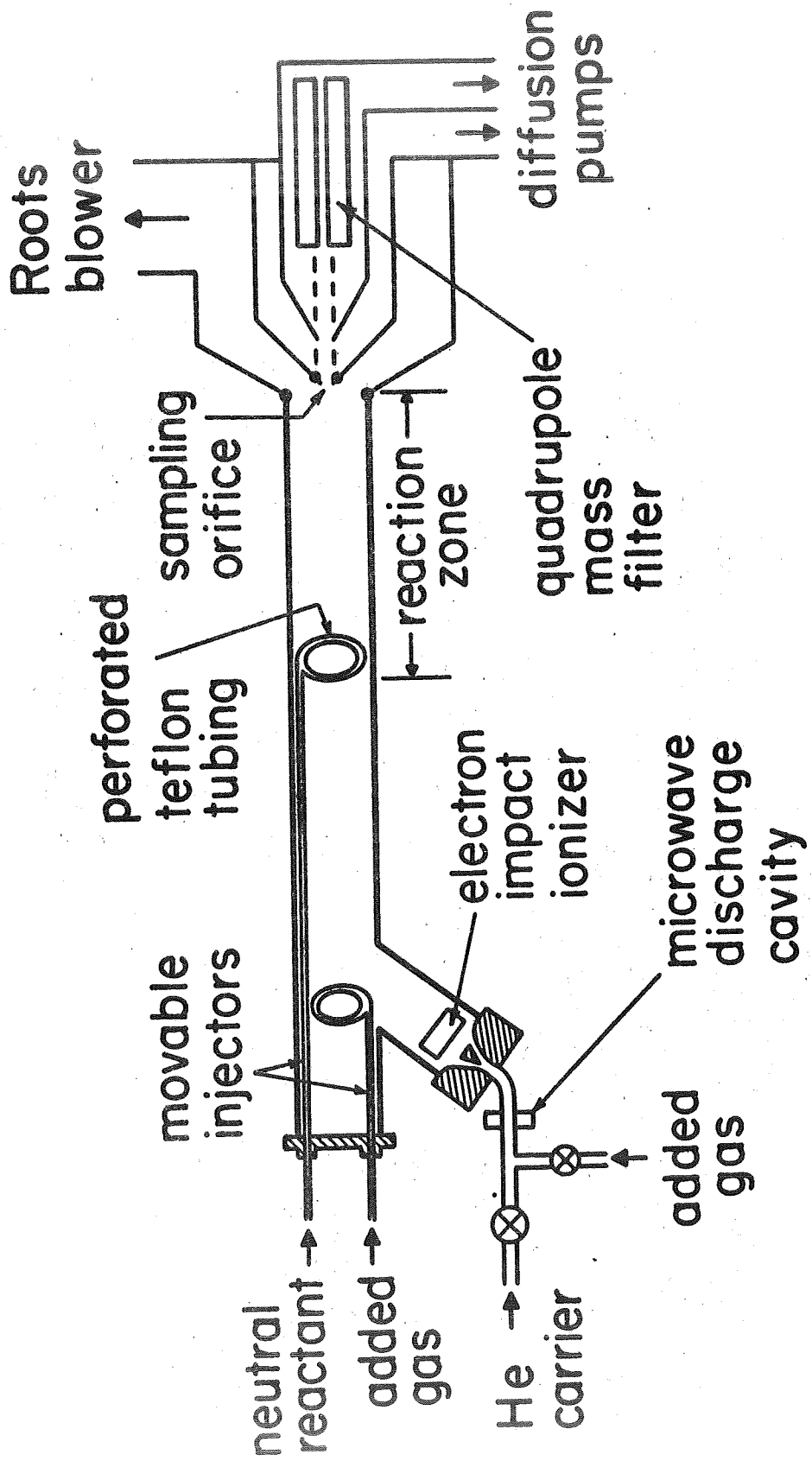


Figure 1. Diagram of apparatus.

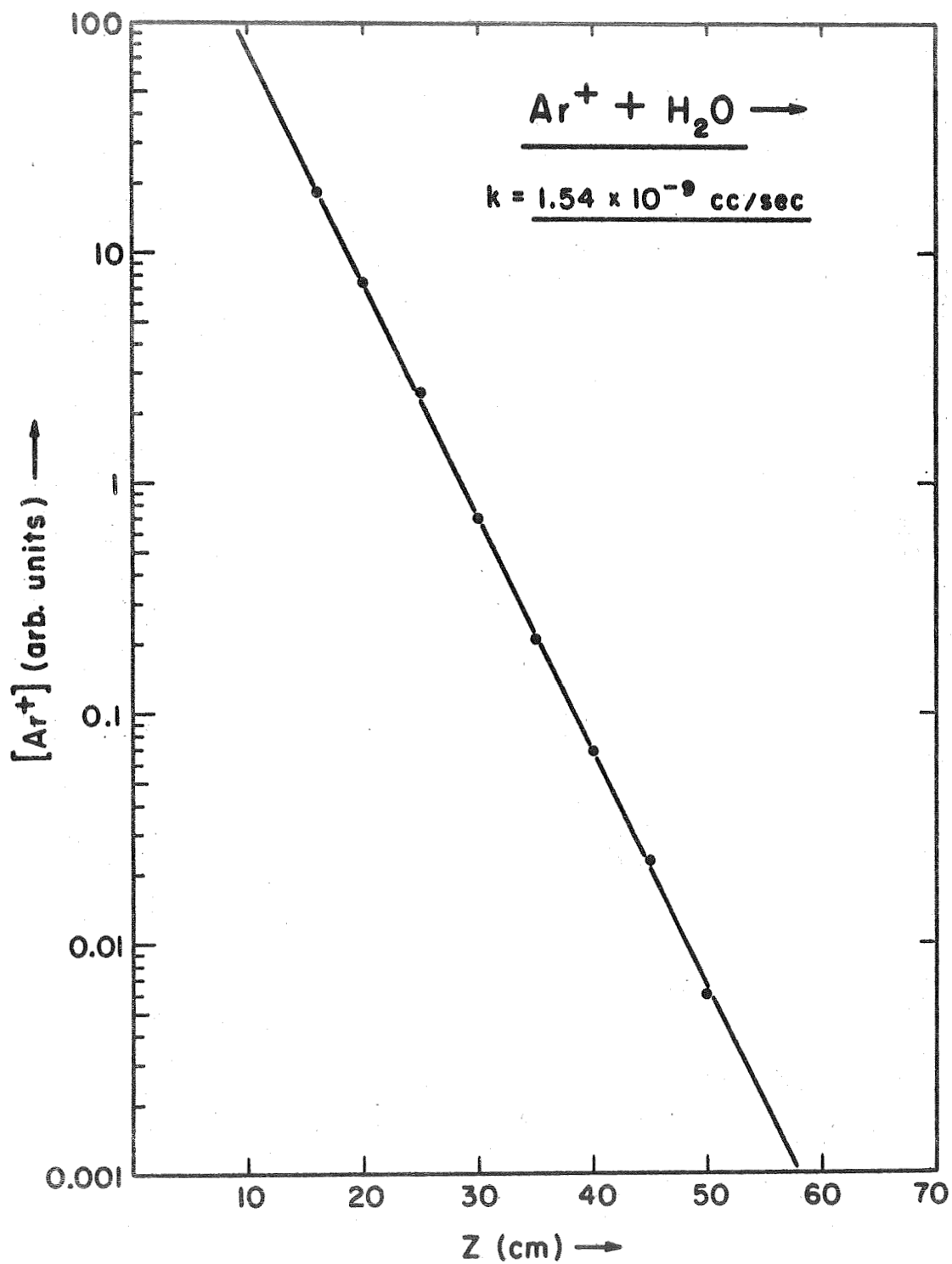


Figure 2.  $\text{Ar}^+$  current vs. position of movable injector at constant  $\text{H}_2\text{O}$  flow. ( $P_{\text{He}} = .57$  torr,  $P_{\text{Ar}} = .04$  torr,  $P_{\text{H}_2\text{O}} = 4.3 \times 10^{-5}$  torr,  $\bar{v} = 6.1 \times 10^3$  cm/sec).

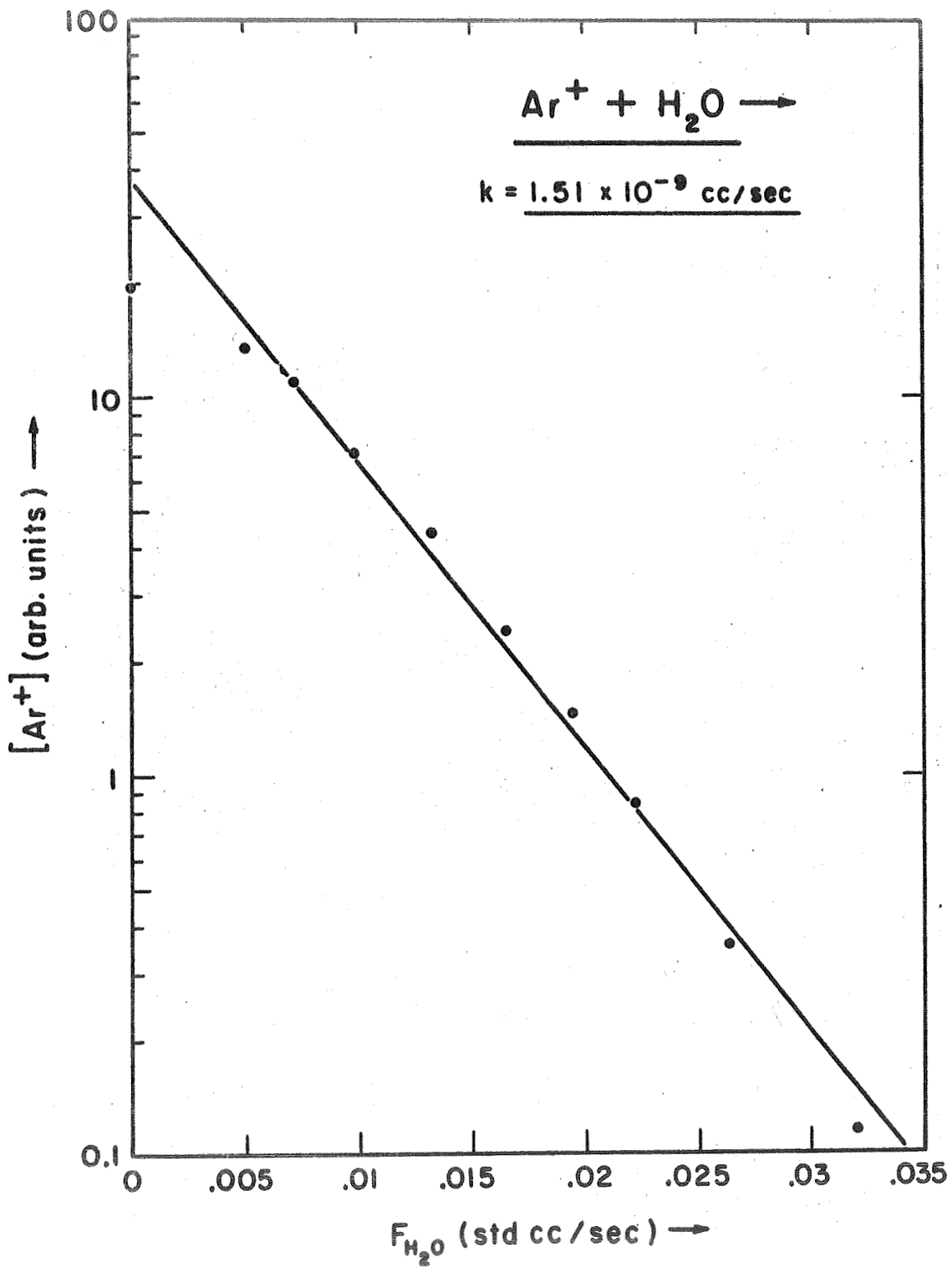


Figure 3.  $\text{Ar}^+$  current vs  $\text{H}_2\text{O}$  addition with  $z = 30$  cm. ( $P_{\text{He}} = .30$  torr,  $P_{\text{Ar}} = .05$  torr,  $\bar{v} = 7.9 \times 10^3$  cm/sec.)



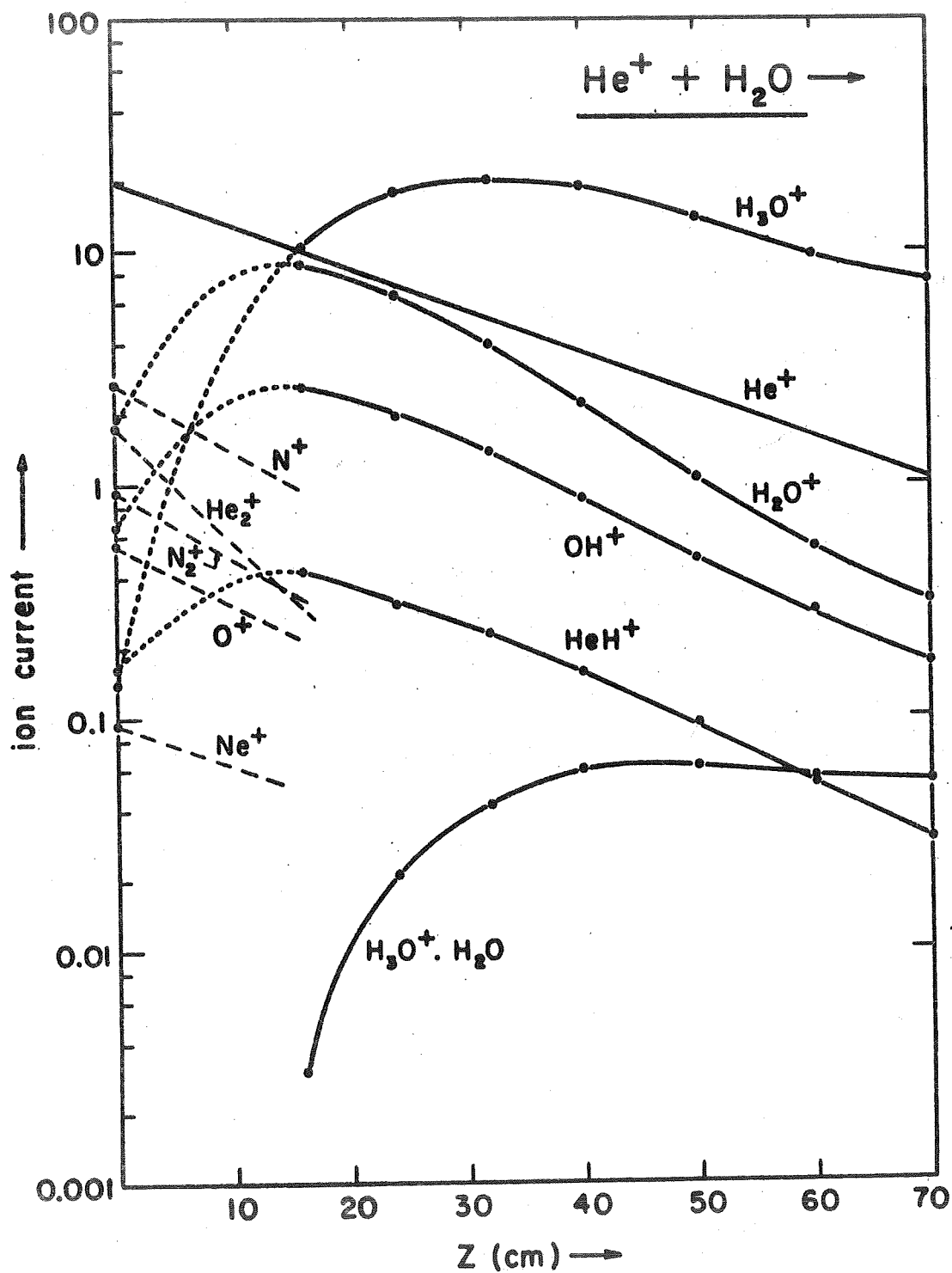


Figure 4. Ion currents vs. position of movable injector. ( $P_{\text{He}} = .35$  torr,  $P_{\text{H}_2\text{O}} = 1.8 \times 10^{-5}$  torr,  $\bar{v} = 9.6 \times 10^3$  cm/sec).

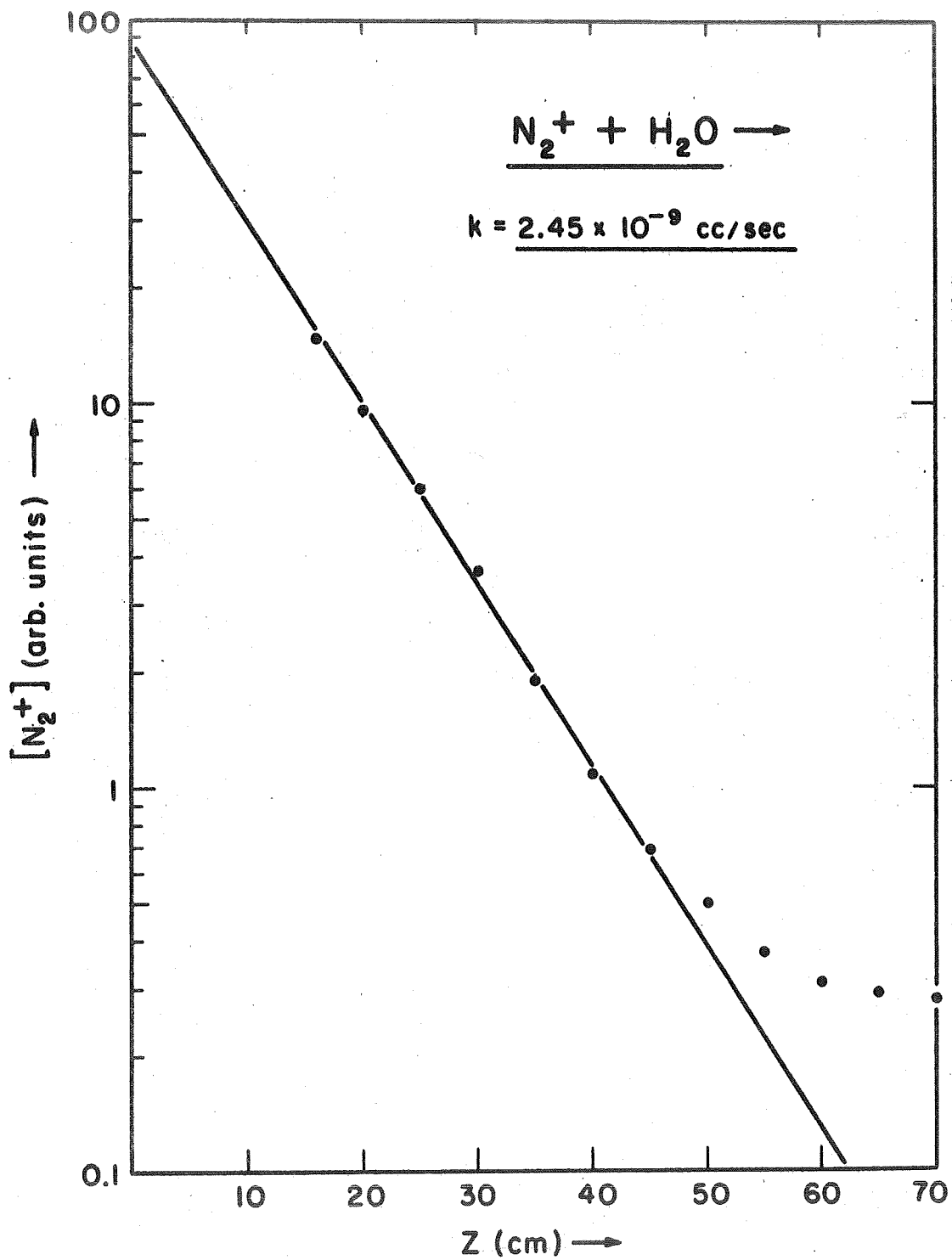


Figure 5.  $N_2^+$  current vs. position of movable injector. ( $P_{He} = .44$  torr,  $P_{N_2} = .004$  torr,  $P_{H_2O} = 2.0 \times 10^{-5}$  torr,  $\bar{v} = 9.4 \times 10^3$  cm/sec).